



PERGAMON

Available online at www.sciencedirect.com

SCIENCE @ DIRECT®

International Journal of
MECHANICAL
SCIENCES

International Journal of Mechanical Sciences 45 (2003) 373–396

www.elsevier.com/locate/ijmesci

Modelling metal cutting using modern ductile fracture mechanics: quantitative explanations for some longstanding problems

A.G. Atkins*

Department of Engineering, University of Reading, Box 225, Reading RG6 6AY, UK

Received 23 May 2001; received in revised form 6 June 2002; accepted 29 January 2003

Abstract

The assumption that negligible work is involved in the formation of new surfaces in the machining of ductile metals, is re-examined in the light of both current Finite Element Method (FEM) simulations of cutting and modern ductile fracture mechanics. The work associated with separation criteria in FEM models is shown to be in the kJ/m^2 range rather than the few J/m^2 of the surface energy (surface tension) employed by Shaw in his pioneering study of 1954 following which consideration of surface work has been omitted from analyses of metal cutting. The much greater values of surface specific work are not surprising in terms of ductile fracture mechanics where kJ/m^2 values of fracture toughness are typical of the ductile metals involved in machining studies. This paper shows that when even the simple Ernst–Merchant analysis is generalised to include significant surface work, many of the experimental observations for which traditional ‘plasticity and friction only’ analyses seem to have no quantitative explanation, are now given meaning. In particular, the primary shear plane angle ϕ becomes material-dependent. The experimental increase of ϕ up to a saturated level, as the uncut chip thickness is increased, is predicted. The positive intercepts found in plots of cutting force vs. depth of cut, and in plots of force resolved along the primary shear plane vs. area of shear plane, are shown to be measures of the specific surface work. It is demonstrated that neglect of these intercepts in cutting analyses is the reason why anomalously high values of shear yield stress are derived at those very small uncut chip thicknesses at which the so-called size effect becomes evident. The material toughness/strength ratio, combined with the depth of cut to form a non-dimensional parameter, is shown to control ductile cutting mechanics. The toughness/strength ratio of a given material will change with rate, temperature, and thermomechanical treatment and the influence of such changes, together with changes in depth of cut, on the character of machining is discussed. Strength or hardness alone is insufficient to describe machining. The failure of the Ernst–Merchant theory seems less to do with problems of uniqueness and the validity of minimum work, and more to do with the problem not being properly posed. The new

* Corresponding author. Tel.: +44-118-931-8562; fax: +44-118-931-3327.

E-mail address: a.g.atkins@reading.ac.uk (A.G. Atkins).

analysis compares favourably and consistently with the wide body of experimental results available in the literature. Why considerable progress in the understanding of metal cutting has been achieved without reference to significant surface work is also discussed.

© 2003 Elsevier Science Ltd. All rights reserved.

1. Introduction

Astakhov [1] points out that there is a major difference between machining and other metal forming processes, in that there must be physical separation of the layer to be removed from the work material, and that the process of separation forms new surfaces. Shaw [2] in his pioneering studies of machining was the first to consider whether the energies associated with chip momentum change and with the formation of new surfaces were likely to be as significant as the components of total work in cutting associated with chip plastic flow and friction. He calculated that the inertial item was negligible under normal conditions of cutting and, using chemical surface free energy values of a few J/m^2 for the work to create new surfaces, concluded that work was negligible too. That view has been the received wisdom ever since, and subsequent ‘algebraic’ (as opposed to Finite Element) analyses of metal cutting have involved plasticity and friction only.

This paper will demonstrate that metal cutting is, in fact, from the class of ductile fracture problems where there is complete plastic collapse (in the formation of the chip). Slip line field, and similar analyses of chip flow calculate only this collapse work of so-called ‘remote flow’ and omit the toughness work in the highly deformed boundary layers contiguous with the machined surface. That the toughness work is appreciable is backed by calculations from finite element method (FEM) simulations of cutting given later. A new algebraic model for cutting which incorporates significant surface work will be presented which explains quantitatively a number of experimental observations for which present machining theories seem to have no explanation.

The growing body of FEM simulations of machining, on the face of it, consider only plasticity and friction but, unlike traditional algebraic models, it is found that a *separation criterion* has to be employed at the tool tip in order to permit tool movement. Such criteria remain today an essential part of FEM analyses for continuous and discontinuous chip formation (e.g. [3]). In conventional plastic flow, neighbouring material elements remain neighbours after deformation and neither algebraic nor FEM models of bulk forming or sheet forming require special additional criteria for their solution. The requirement for the extra separation criterion in FEM models of cutting relates to the difference between cutting and conventional plastic flow, highlighted above, namely the formation of new surfaces: material elements just above, and just below, the putative parting line become separated, some going away to form the undersurface of the chip, some going to form the highly-distorted thin surface layer of the cut body in which residual stresses are found (e.g. [4–6] Liu and Guo, 2000). Without a separation criterion, the problem is that of elastoplastic inclined indentation near the corner of a block of material.

So long as the work of forming new surfaces is negligible, *any* separation criterion could seemingly be employed in FEM cutting models, and the requirement could be viewed as a ‘computational fix’ to cope with the singularity at the sharp tip of the tool. It is indeed the case that a wide variety of separation criteria has been employed in the elements around the tool tip, including a critical

von Mises strain [5–8] a critical strain energy density [9]; a distance tolerance [10,11] in which category comes the ‘fictitious wedge at the tool tip’ used by Usui and Shirakasi [12]; conditional link elements, Zhang and Bagchi [13]; a critical stress at a critical distance (cleavage in steel) and a hydrostatic-stress dependent critical strain (ductile separation in steel) both used by Marusich and Ortiz [14]. Even though all these criteria have permitted FEM programs to run, the ‘best’ to employ is, presumably, that most closely representing the physics of what goes on at the tool tip. Certainly residual stress distributions in the machined layer, and the distributions of effective plastic strain both in the chip and machined surface, depend on the criterion employed, Huang and Black [15].

All these separation criteria must have work associated with them which is performed in the material elements along the parting line. To assess whether the surface free energy is the correct parameter by which to judge whether surface work is negligible, it is important to know the magnitude of the FEM separation work. It is not reported in any of the FEM machining papers but it may be calculated—at least for those criteria having some physical meaning. When a critical strain energy density criterion (critical plastic work per volume) or critical von Mises strain is employed, the separation work/volume may be converted into a critical work/area by multiplying by the size of the elements to which the separation criterion is applied [16]. Strenkowski and Carroll [7] employed a critical von Mises strain of $\varepsilon = 0.6$ for the solution heat treated and cold worked 2024-T361 aluminium alloy having a yield strength of some 450 MPa. The separation criterion as a critical work/volume is therefore $450 \times 10^6 \times 0.6 = 270 \text{ MJ/m}^3$ for the elements at the crack tip. The thickness of the elements (or, equivalently, the highly distorted boundary layer on the underside of the chip and surface of the cut body) is some $30 \mu\text{m}$ or less, whence the work done per unit area in the surface layer becomes some 8 kJ/m^2 . This is far different from the chemical surface free energy of a few J/m^2 . Lin and Lo’s [9] critical strain energy density for cutting mild steel is some 700 MJ/m^3 with element size $33 \mu\text{m}$, giving 23 kJ/m^2 ; from Liu and Guo’s 2000 data, and Yang and Liu’s 2002 data, for cutting annealed 304 stainless steel, the separation specific work is some $13\text{--}53 \text{ kJ/m}^2$. Calculations from other authors’ data for other materials, e.g. Marusich and Ortiz [14], also suggest kJ/m^2 for the work to form the new surfaces. Such specific separation work is some 5–20% of the total work rates for cutting predicted by these different FEM simulations, (predicted cutting forces of about 250 N/mm and cutting speed of 3 m/s in the case of Liu and Guo [6], for example). What does all this mean for traditional ‘algebraic’ metal cutting analyses which do not incorporate significant surface work? And why is it that considerable progress in the understanding of chip flow, chip curl, built-up edge formation, tool stresses and tool temperatures etc. has been made over the past half-century without regard to work of surface separation?

The discrepancy in surface work values is not surprising in terms of modern fracture mechanics. Although Griffith employed surface free energies in his seminal work on glass [17,18] as did Obreimoff [19] when cleaving mica, Orowan and Irwin in the 1940s showed that the specific work of fracture (work/area or ‘fracture toughness’), which determines the forces and work for material separation, is in most cases at least three orders of magnitude greater than the surface free energy (see [20]). The practical specific work of fracture, or ‘specific essential work of fracture’, given the symbol R , is much greater than the surface free energy owing to the zone of irreversible work at the crack tip (which exists even in brittle fracture), which then forms the severely deformed thin boundary layers alongside the new surfaces as separation proceeds. In ductile metals the specific works of fracture are even greater at 10s or 100s of kJ/m^2 (they are the so-called J_C or even J_R values see, for example, [21]). These values of kJ/m^2 may be independently calculated using models

of void growth and coalescence which is the microstructural process by which separation is achieved and new surfaces formed in commercial ductile metals (see, for example, [22,23]). Satisfaction of a separation criterion at the tool tip in FEM models of machining is exactly the same as the use today of ‘cohesive zone models’ or ‘porous plasticity damage mechanics’ to predict ductile fracture in elastoplastic structural integrity assessments (e.g. [24]).

Chemical surface energy is a short-range parameter [25] and both the size of the microstructural regions in which separation by voiding occurs (the thickness of the thin highly deformed boundary layers), and the surface roughnesses produced by voiding, are at least an order of magnitude greater than the range over which the forces associated with the chemical surface energy parameter act. Indeed, Bickerman [26] was critical of the concept of solid (as opposed to liquid) surface energy because the surfaces of solids are elastic or plastic, and the associated forces are so large that they dominate the surface tension, thus making solid surface energy extremely difficult to measure. This again suggests that chemical surface energy is not the correct parameter to employ in machining.

Nevertheless, there is a reluctance among metal cutting practitioners to contemplate that cracking and fracture, and the associated work, can have anything to do with the *continuous-chip* machining of ductile metals because free-standing cracks are not observed at tool tips in normal machining. Whether free-standing cracks run ahead of the tool in machining is actually an entirely different question from that of satisfying the conditions for surface separation, as it concerns crack *stability*. In FEM simulations of cutting with free-standing cracks, the separation criterion would be satisfied in numbers of elements ahead of the tool tip. Tool tip cracking *can* happen in ‘less ductile’ materials being cut under ‘abnormal conditions’ such as at large depths of cut, with large positive rake angles and so on. Then the ‘surface formation’ (crack) speed is faster than the tool speed. In ‘normal’ machining there are no free-standing cracks at the tool because the tool speed and ‘surface formation’ speed coincide. Cracking ahead of the tool certainly happens in cropping and bar shearing when a bar is severed by a punch, the stroke of which is less than the thickness of the bar; but cropping of other materials sometimes requires the full stroke of the punch. Such differences can only be explained when the additional parameter of material toughness is employed in the analysis as well as flow stress (e.g. [27]). The mechanics of guillotining are not really different in principle from machining: the ‘far boundary’ is much closer so that the collapse plasticity occurs in a shear bands across the whole thickness rather than in chip deformation.

It is also important to comment at this stage that the formation of *discontinuous* chips, by possible shear fracture along the primary shear plane, is also an entirely different problem from the need to create new machined surfaces in cutting. Shaw [28] proposed a new mechanism for plastic flow at large strains to take account of the formation/rehealing/coalescence of hidden microcracks in shear and its effect on cutting. A strong influence of hydrostatic stress on the initiation of cracking across the primary shear plane featured in the analysis, as it does in all microstructural void-growth models. Shaw’s approach complements the different line of attack of ductile fracture mechanics to large deformation problems employed in this paper, in which the energy for cracking is separated from that for gross plastic flow. The whole question of different types of chip (including elastically fractured chips in cutting brittle materials) and the transitions between their formation will be the topic of another paper, in which it will be demonstrated that the cutting mechanics presented here apply to materials as diverse as wood and plastics. For present purposes, the important realisation from the FEM simulations of cutting discussed above, and from the physics of the problem, is that surface (fracture) work can be significant in machining even when no obvious cracking is evident.

Ductile separation involves both work local to the crack surfaces and ‘remote’ work which produces gross permanent deformation in all, or part, of the body away from the new surface. Metal-cutting belongs to the class of ductile fracture problems where there is complete plastic collapse, i.e. in the formation of the chip. The plastic work of chip formation in cutting is the ‘remote’ work and it is this component (*only*) of total ductile work that conventional metal cutting theories evaluate using slip line fields etc. (along, of course, with frictional effects). As discussed in Section 2 later, since traditional machining models are based on a force equilibrium approach, rather than a work analysis, it will not have been evident that a component of total work done has been omitted. (Recall that in traditional metal forming analyses friction, in particular, and to a lesser degree rate- and temperature-dependent flow strengths, are often employed as disposable parameters to make ‘theory’ and experiment agree. In FEM modelling the question of surface work cannot be avoided owing to the requirement for a separation criterion.)

This paper will show that incorporation of significant surface work in even the simplest of algebraic machining theories gives very satisfying results which agree with continuous-chip machining experiments and which remove many of the shortcomings of traditional approaches. Firstly, the primary shear plane angle ϕ becomes material-dependent (since there are now two independent material parameters, namely the yield strength and the surface specific work). The new analysis predicts when quasi-linear relations between cutting forces and uncut chip thickness, as often found experimentally in both orthogonal and oblique machining, are to be expected. Also predicted are the positive force intercepts (called the ‘force unavailable for chip deformation’ by Kobayashi and Thomsen [29]) which are found experimentally in such plots but usually ignored in subsequent analysis of data. The existence of a force intercept also provides an explanation for the so-called ‘size effect’ in metal cutting. The new theory shows how cutting tests may be employed to determine not only the yield strength of the metal being cut but also its toughness.

While the present model quantitatively displays all the features of interest, there is no doubt that improvements would be gained by employing more complicated flow fields and a better representation of friction. It is noteworthy that McClintock [30] has recently introduced a new field of study called ‘slip line field fracture mechanics’. Metalcutting could usefully be modelled using this line of attack.

2. Model

We keep to the straightforward upper bound single shear plane model with Coulomb friction. It is fully appreciated that there are greatly improved models of chip flow and tool-chip friction (for a review, see [5]) but the following analysis displays remarkably well all the features of importance. Fig. 1 shows the geometry of orthogonal cutting and the nomenclature. Piispanen [31] introduced the well-known ‘deck of cards’ model for the way in which material to be removed was sheared into the chip and the ideas appear in the Ernst–Merchant analysis (as early as 1881 Mallock had demonstrated that cutting took place by shear [32]). Cook et al. [33, p. 156] realised that it was impossible for the Piispanen model to operate in plane plastic strain at constant plastic volume without there being ‘new surface’ at the tip of the tool, i.e. there had to be a ‘gap’ of at least the thickness of the shear band which released material to be sheared. Few, if any, subsequent authors of monographs on machining have remarked on this percipient observation when introducing basic

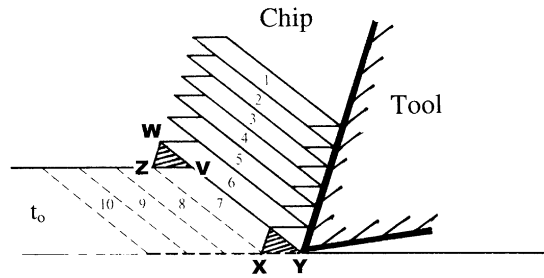


Fig. 1. Piispanen's 'deck of cards' model. If slip occurs in plane strain in a finite width band along the primary shear plane, plastic volume cannot be conserved unless a gap occurs in the region of XY . Otherwise ZWV is an increase in plastic volume (adapted from Cook et al. [33]).

cutting mechanics, presumably because they share the belief that the work of creating the gap is negligible so that plasticity and friction analyses will provide adequate models.

When surface work is significant during steady deformation, there will be internal work of (i) plasticity along the shear plane; (ii) friction along the underside of the chip at the tool interface; and (iii) formation of new cut surface. All this work is provided externally by the component F_C of the tool force moving parallel to the machined surface. Hence

$$F_C V = (\tau_y \gamma)(t_0 w V) + [F_C \sec(\beta - \alpha) \sin \beta] \frac{V \sin \phi}{\cos(\phi - \alpha)} + R w V, \quad (1)$$

where V is the cutting velocity, F_C is the horizontal component of the cutting force, τ_y is the (rigid-plastic) shear yield stress, γ is the shear strain along the shear plane, given by $\gamma = \cot \phi + \tan(\phi - \alpha) = \cos \alpha / \cos(\phi - \alpha) \sin \phi$, t_0 is the uncut chip thickness, w is the width of the orthogonal cut, β is the friction angle given by $\tan \beta = \mu$, with μ the coefficient of friction, α is the tool rake angle, ϕ is the orientation of the shear plane and R is the specific work of surface formation (fracture toughness).

The three terms on the rhs of Eq. (1) represent in order components (i)–(iii) above. The friction force in (ii) is obtained from the Merchant force circle in the usual way. The component of the cutting force vertical to the cut surface F_V (which does no work) is also given from the force circle, namely

$$F_V = F_C \tan(\beta - \alpha). \quad (2)$$

From Eq. (1) we obtain

$$\frac{F_C}{w \tau_y t_0} = \frac{\cos(\beta - \alpha)}{\sin \phi \cos(\phi + \beta - \alpha)} \left[1 + \frac{R \cos(\alpha - \phi) \sin \phi}{\tau_y t_0 \cos \alpha} \right] \quad (3)$$

using $\gamma = [\cos \alpha / \cos(\phi - \alpha) \sin \phi]$ and manipulating the trig functions. When the second term in the square brackets is zero, Eq. (3) derived on the basis of work corresponds with the force-balance Ernst–Merchant theory (see, for example, Eq. (2.16) in Boothroyd [34]). Eq. (3) cannot be obtained from an equilibrium approach.

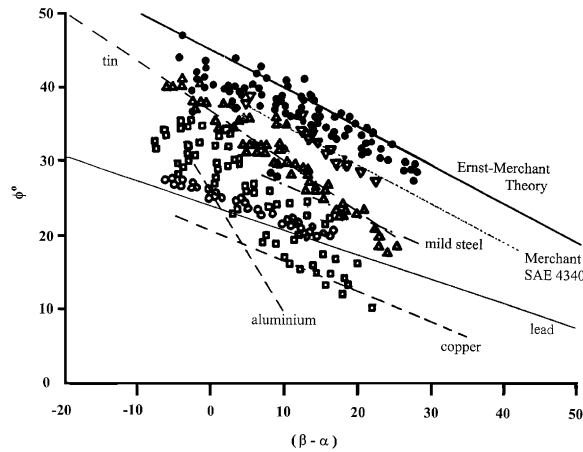


Fig. 2. Experimental data for shear plane angle ϕ and $(\beta - \alpha)$ where β is the friction angle along the rake face and α is the tool rake angle. The data points are from Eggleston et al. [46] and the lines are empirical correlations by Pugh [38] for various materials, the host of data points for which are not shown to avoid confusion. Diagram adapted from Oxley [42].

Merchant [35] argued that ϕ adjusts itself so that the total work rate (or F_c) is a minimum which gives (using the first term only on the rhs of Eq. (3))

$$\phi = (\pi/4) - (1/2)(\beta - \alpha). \quad (4)$$

Subject to different β , this prediction should apply to *all* materials irrespective of their different mechanical properties. It is well known that this prediction for ϕ fails to give quantitative agreement with experiment for ductile metals. The only materials investigated by Merchant [36] for which predictions of ϕ came close to experiment were relatively brittle synthetic plastics which nevertheless displayed some ductility: (cutting really brittle materials at the depths of cut employed in metal cutting simply ‘knocks lumps out’ of the material and produces severe sub-surface cracking). Fig. 2, plotted in the form of ϕ vs. $(\beta - \alpha)$ popularised by the Merchant line of attack, shows that most experimental data for ductile metals lie below the minimum work prediction. Furthermore it seems clear from Fig. 2 that ϕ is material-dependent (which is *not* predicted by the Merchant analysis) and, indeed, a number of authors have given empirical relations between the experimental ϕ and $(\beta - \alpha)$ for a wide range of different materials (see [37]). For example, Pugh [38] gives

$$\phi + c_1(\beta - \alpha) = c_2 \quad (5)$$

where c_1 and c_2 are material-dependent constants.

The failure of the simple theory to describe the experimentally observed material-dependent ϕ values called into question the validity of applying minimum work arguments to the cutting problem, since the shape of the free surface of the chip is unknown and must form part of the solution [39,40]. But we show in this paper that minimisation is perhaps not the cause of the failure of the original Ernst–Merchant model. Rather failure of the Ernst–Merchant model when applied to ductile materials is because the problem was not properly posed in the first place (i.e. did not contain the surface work term). Furthermore we shall show that sensible material-dependent predictions for ϕ are obtained

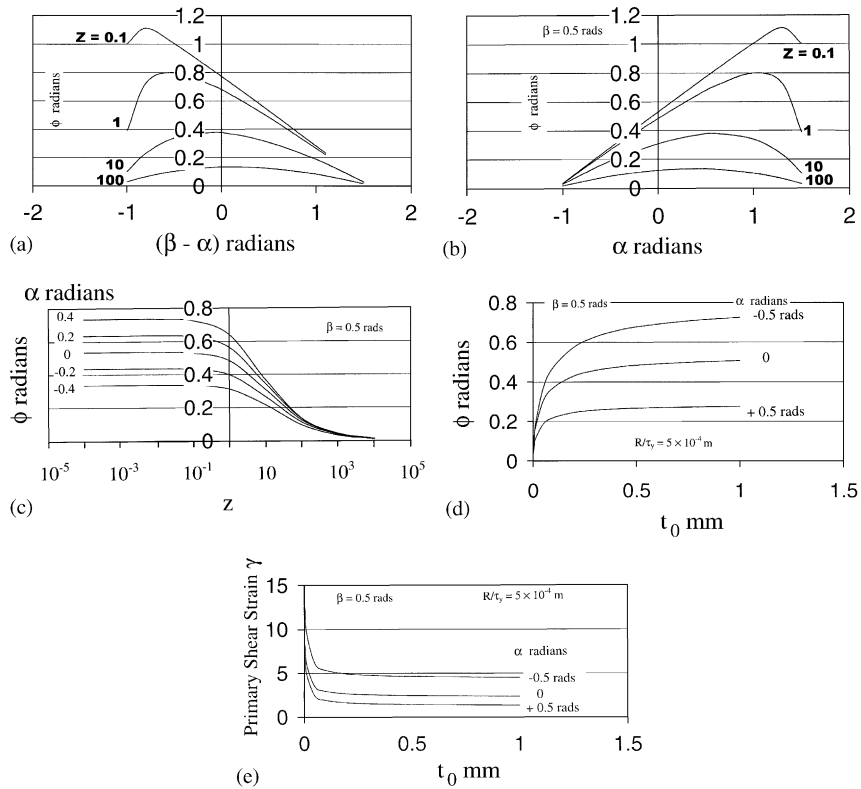


Fig. 3. (a) Predictions of the new analysis for ϕ vs. $(\beta - \alpha)$. Values depend upon $Z = R/\tau_y t_0$. The diagram relates to $\beta = 29^\circ$. Increasing friction lowers all the curves and vice-versa. (b) Predictions of the new analysis for ϕ vs. α at constant Z and constant β . Increasing friction lowers all the curves and vice-versa. (c) Predictions of the new analysis for ϕ vs. Z at constant α and β . Increasing friction lowers all the curves and vice-versa. (d) Variation of ϕ with α , β and R/τ_y . Increasing friction lowers all the curves and vice-versa. For greater R/τ_y , curves take greater t_0 before levelling-out and vice-versa. (e) Variation of shear strain γ on primary shear plane with t_0 at various α , β and R/τ_y . For greater R/τ_y , curves take greater t_0 before levelling-out and vice-versa.

when proper magnitudes of separation work are incorporated in the minimisation. Stephenson and Agapiou [41, p. 471] have a detailed discussion about minimum work and uniqueness assumptions applied to the cutting problem and they conclude that minimum work is an acceptable line of attack.

By differentiating the whole of Eq. (3) it may be shown that ϕ for least F_c satisfies

$$\left[1 - \frac{\sin \beta \sin \phi}{\cos(\beta - \alpha) \cos(\phi - \alpha)} \right] \left[\frac{1}{\cos^2(\phi - \alpha)} - \frac{1}{\sin^2 \phi} \right] = - [\cot \phi + \tan(\phi - \alpha) + Z] \left[\frac{\sin \beta}{\cos(\beta - \alpha)} \left\{ \frac{\cos \phi}{\cos(\phi - \alpha)} + \frac{\sin \phi \sin(\phi - \alpha)}{\cos^2(\phi - \alpha)} \right\} \right] \quad (6)$$

in which $Z = R/\tau_y t_0$ is the parameter which makes ϕ material dependent. Eq. (6) is solved numerically.

Fig. 3a plots some predictions from solution of Eq. (6) in the ϕ vs. $(\beta - \alpha)$ form. Instead of the single “ $\phi = (\pi/4) - (1/2)(\beta - \alpha)$ ” line, we now have a series of lines depending on Z .

For fixed β , increasing Z lowers ϕ ; and for fixed Z , increasing β also lowers ϕ . We observe straight away that the Z - and β -dependent ϕ vs. $(\beta - \alpha)$ loci fall below the Merchant line precisely in the region where experimental data lie, cf. Fig. 2. Comparison with experimental data is made in Section 3.1. The present analysis collapses into the Ernst–Merchant line for $Z = 0$. The value of the non-dimensional parameter Z when predictions for ϕ move significantly away from the Ernst–Merchant line is round about unity, but actually depends upon the friction angle β . The higher the friction, the lower the Z at which differences appear between the solution of Eq. (6) and the Ernst–Merchant prediction. This is more easily seen from the next graph, Fig. 3b which gives ϕ vs. α for constant Z and constant β . For $Z = 0$, the ϕ – α relationship is the same straight line as the Ernst–Merchant frictionless solution, i.e. $\phi = \pi/4 + \alpha/2$. For finite Z , ϕ is virtually linear with α over a limited range (cf. Pugh’s relation in Eq. (5)). The range of α diminishes as Z increases.

Now Z is a parameter that involves both the material property R/τ_y and the uncut chip thickness t_0 . Hence, for a given material, as t_0 changes so does Z and ϕ should vary with t_0 according to Figs. 3a and b. There is debate in the metal cutting literature as to whether experimental ϕ do vary with depth of cut, e.g. Oxley [42]. Fig. 3c, which plots ϕ vs. Z at fixed α and fixed β , provides the answer to that question. At sufficiently small Z (below a threshold of $10^{-1} \sim 10^{-2}$ say), ϕ is independent of Z , which means that for a given material R/τ_y , ϕ is independent of t_0 once t_0 is bigger than about $(10 R/\tau_y)$; conversely ϕ will become progressively smaller at smaller depths of cut. Fig. 3d shows how ϕ varies with t_0 at various rake angles α , friction angles β , and material R/τ_y . The constancy of ϕ at small Z means that, in Figs. 3a and b, loci of constant $Z < 10^{-1}$ are also loci of constant ϕ ; that is not the case for loci of larger Z .

At those depths of cut where ϕ is constant, the primary shear strain γ is then also constant for given tool angle α , Fig. 3e, but at very small t_0 , γ increases. At these small depths of cut that put Z over the threshold value of about 0.1 and where ϕ decreases and γ decreases, the so-called ‘size effect’ in metal cutting occurs (see Section 3.3 later).

We may rewrite Eq. (3) as

$$F_c = \left(\frac{\tau_y w \gamma}{Q} \right) t_0 + \frac{Rw}{Q}, \quad (7)$$

where Q is the friction correction given by

$$Q = [1 - (\sin \beta \sin \phi / \cos(\beta - \alpha) \cos(\phi - \alpha))]. \quad (8)$$

The bracketted term in Eq. (7) is constant when t_0 is big enough to make $Z = R/\tau_y t_0 < \text{about } 0.1$, because γ is then constant, Fig. 3e. Hence, under these conditions F_c is predicted to vary linearly with t_0 , the plot having a positive force intercept which is a measure of the specific surface work (material toughness). The Q value for the intercept is that given by Eq. (8) employing the appropriate levelled-out ϕ value at large t_0 . Positive force intercepts of cutting force vs. uncut chip thickness are found experimentally for which a variety of explanations have been put forward including flank wear, rubbing on the clearance face of the tool, and bulging ahead of the tool (see the various monographs given in the references). The positive force intercept is usually ignored in analyses of cutting data. Brown and Amarego [43] calculate the uncertainties caused by the effect of including, or subtracting, the intercepts in calculations of chip flow angles in oblique machining. The new analysis of cutting in this paper says that the intercepts are to be expected and that estimates of material toughness may be derived from them (see Section 3.2 later). The linear prediction of

Eq. (7) is reminiscent of the ‘essential work of fracture’ analysis to separate local from remote work in ductile fracture, propounded by Cotterell and coworkers (for a review, see Chapter 4 of [44]).

At very small t_0 at which neither ϕ nor γ is constant, the F_C vs. t_0 plot becomes non-linear and concave-downwards. Even so, it does *not pass through the origin* and still has a force intercept given by Rw/Q where now $Q(=1)$ is the value calculated for $t_0=0$ (see Section 3.2 later). In other words, even though F_C vs. t_0 is not linear at small t_0 , the intercept still gives Rw because, although the non-essential work of fracture is not exactly proportional to t_0 since ϕ depends on t_0 in this range, the essential work of fracture rate is simply RwV .

The specific cutting pressure (‘unit power’) F_C/wt_0 follows from Eq. (7) i.e.

$$\frac{F_C}{wt_0} = \frac{\tau_y \gamma}{Q} + \frac{R}{Q} \left[\frac{1}{t_0} \right], \quad (9a)$$

$$= \frac{\tau_y}{Q} (\gamma + Z). \quad (9b)$$

At sufficiently large t_0 which put Z below the threshold value of about 0.1, γ is constant and the unit power is essentially constant, Eq. (9b), since $\gamma \gg 0.1$. At small t_0 and larger Z where γ increases, the unit power increases markedly (cf. the inverse relationship with t_0 in Eq. (9a)). This phenomenon is the so-called size effect in machining. As with the positive force intercept in plots of F_C vs. t_0 , various explanations have been put forward for the size effect, including the reduced statistical chance of encountering flaws or microcracks at the very small depths of cut involved, but the present analysis expects it to occur.

The shear force F_S along the shear plane is obtained by resolving F_C and F_V to give

$$\begin{aligned} F_S &= F_C \cos \phi - F_V \sin \phi, \\ &= [1/Q][\cos \phi - \tan(\beta - \alpha) \sin \phi][\tau_y \gamma \sin \phi A_S + Rw] \\ &= \left[\frac{\cos[(\phi - \alpha) + \beta] \cos \alpha}{[\cos(\beta - \alpha) \cos(\phi - \alpha) - \sin \beta \sin \alpha]} \right] \tau_y A_S \\ &\quad + \left[\frac{\cos[(\phi - \alpha) + \beta] \cos(\phi - \alpha)}{[\cos(\beta - \alpha) \cos(\phi - \alpha) - \sin \beta \sin \alpha]} \right] Rw, \end{aligned} \quad (10)$$

where $A_S = wt_0/\sin \phi$ is the area of the shear plane. For $\alpha = 0$, this takes the very simple form

$$F_S = \tau_y A_S + \cos \phi Rw, \quad (11)$$

which remarkably is independent of Q and which is a linear variation of F_S with A_S , with a slope giving τ_y and intercept giving $Rw \cos \phi$ (the ϕ value for which is the levelled-out value at large t_0). For finite α the algebra of Eq. (10) does not simplify, but calculations show that for positive and negative rake angles in the practical range, the differences between the ‘full’ Eq. (10) and the simple Eq. (11) are relatively small. Furthermore, as found experimentally, F_S vs. A_S plots are comparatively insensitive to changes in α . The changes in ϕ with α for typical ductile metals are also small, so the plot in practice has a ‘single intercept’.

As with F_C vs. t_0 plots, F_S vs. A_S plots curve down towards the origin at very small t_0 , but still have a positive force intercept.

3. Comparison with experiment

3.1. Primary shear plane angle ϕ

Fig. 4 is from Okoshi [45]. It shows the shear plane angle ϕ vs. rake angle α . The curves replicate those in Fig. 3b, and satisfyingly show the peaking of ϕ at large tool rake angles. Calculations show that the Z values are about: 2–5 for cast iron; 5–7 for brass; 17 for aluminium; and 25–30 for mild steel all with $0.25 < \beta < 0.3$. The depths of cut were some 0.1 mm in these particular experiments of Okoshi, whence the material R/τ_y are about: 3×10^{-4} m (cast iron); 6×10^{-4} (brass); 2×10^{-3} (aluminium); and 3×10^{-3} (steel). Such values may be quickly established by performing calculations on a spreadsheet which relates ϕ with α , β and Z from Eq. (6). For yield stresses in the MPa range, these ratios imply toughnesses in the kJ/m^2 range.

Pugh's empirical relation for ϕ , given by Eq. (5), is linear and applies only for the lower right hand corner of Fig. 3a. It cannot represent the curving-over of ϕ at small $(\beta - \alpha)$ predicted in Fig. 3a and illustrated by Okoshi's results in Fig. 4. Furthermore, the new model shows that ϕ can depend on t_0 at sufficiently large Z , which again Pugh's empirical relation (and indeed all other empirical relations for ϕ) does not incorporate. Even so, in the positive $(\beta - \alpha)$ quadrant, it is possible to approximate the results in Fig. 3a by a general equation of the same form as Eq. (5). Also, because at small β all the lines of ϕ vs. $(\beta - \alpha)$ at different Z radiate out from the point $\{\phi=0, (\beta - \alpha)=90^\circ\}$

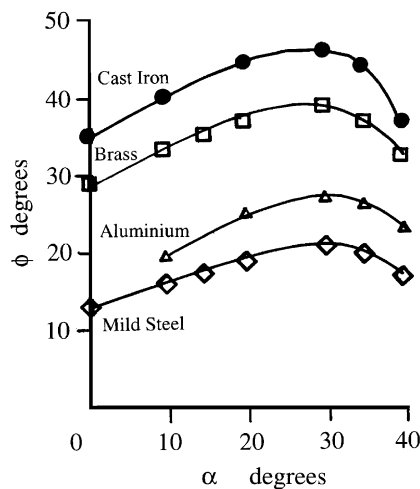


Fig. 4. Okoshi's experimental results from 1929 for changes in the 'direction of slide' (i.e. ϕ) with rake angle. It follows the predictions of Fig. 3b including the peaking of ϕ at large α . (In the original diagram, the 'cutting angle' $\theta = (90 - \alpha)$ was employed in place of α , so the curves were the other way round).

according to the new analysis, c_1 and c_2 are related and we have

$$\phi + c(\beta - \alpha) = c(90^\circ), \quad (5a)$$

where $c = c(Z, \beta)$. For the machining of lead, Pugh gives $\phi + 0.31(\beta - \alpha) = 24^\circ$. Instead of the 24° value for the intercept, we would predict $(0.31)(90^\circ) = 28^\circ$ if we believe the slope; alternatively, if we take the intercept as read, the slope is predicted to be $(24/90) = 0.27$. Both estimates are close. In fact, Pugh's data ought to be replotted in the sense that Eq. (5a) is based on constant Z and constant β . Pugh's experiments employed constant depths of cut for each material, so $Z = R/\tau_y t_0$ is constant, but his β values systematically increased as the tool rake angle α increased (his Fig. 53.18). For example, $18^\circ < \beta < 35^\circ$ as $-20^\circ < \alpha < 60^\circ$ when cutting lead at slow speed. This means that Pugh's data points are rather higher on the left of his ϕ vs. $(\beta - \alpha)$ diagrams, and his empirical slopes rather steeper, than shown in our plots at constant β in Fig. 3a. All this can be accounted for, however, by making up new diagrams of ϕ vs. $(\beta - \alpha)$ from separate plots each having the appropriate β .

Using Pugh's empirical equations for ϕ together with his β values varying with α , it is possible to establish Z for his materials using Eq. (6). We find $Z \approx 17 \sim 30$ (copper); $5 \sim 17$ (lead); $1 \sim 15$ (tin); $4\text{--}9$ (mild steel); $1\text{--}18$ (aluminium). The range of values is similar to that found above for Okoshi's experiments. Using Pugh's depths of cut, $R/\tau_y = Zt_0$ are: $R/\tau_y = 0.003 \sim 0.005$ m (copper); $0.01 \sim 0.02$ m (lead); $0.005 \sim 0.01$ m (tin); $0.0004 \sim 0.0008$ m (mild steel); $0.001 \sim 0.01$ m (aluminium). Again, these data agree with those derived from Okoshi's results. No separate τ_y are given by Pugh or by Okoshi, but from ductile fracture mechanics, the ratios make sense (i.e. R in kJ/m^2 ; τ_y in MPa).

In the comprehensive set of data for ϕ given by Eggleston et al. [46] experiments were done over a range of depth of cut as well as rake angle α . Furthermore, in related papers from the same time (e.g. [29]) force vs. depth of cut data are available for the same materials, which enable ϕ to be calculated by a different route using Eqs. (6) and (10); see next section. Eggleston's et al.'s plots of ϕ vs. $(\beta - \alpha)$ do not distinguish between different depths of cut, all the data points being mixed up as reproduced in Fig. 2 here. In consequence, Z was not constant in the experiments, but that is not important since individual values of Z may be calculated (using a spreadsheet for example) which produce the experimental ϕ for every t_0 employed, using the comprehensive set of tables in Eggleston et al. [46]. Sample calculations for the Z and R/τ_y values give as-received cold rolled 1112 steel ($1 < Z < 5$; $R/\tau_y = 2 \times 10^{-4}$ m); annealed 1112 steel ($2\text{--}10$; 5×10^{-4} m); 2024-T4 aluminium alloy ($0.1\text{--}0.3$; 2×10^{-5} m); 6061-T6 aluminium alloy ($0.1\text{--}0.2$; 1.5×10^{-5}); and 85/15 brass ($1\text{--}5$; 4×10^{-4}). Notice that R/τ_y is smaller for the harder variety of the steel.

3.2. Cutting forces

Another way in which the toughness/strength ratios of materials may be determined is from experimental plots of cutting force F_C vs. depth of cut t_0 , or cutting force resolved along the shear plane F_S vs. the cross-sectional area of the shear plane $A_S = t_0 w/\sin \phi$. A representative example of the former is shown in Fig. 5, taken from Kobayashi and Thomsen [29]. It, like F_S vs. A_S plots aimed to show the constancy of τ_y along the shear plane, has a *positive intercept* at $t_0 = 0$ (and at $A_S = 0$) which is to be expected according to Eqs. (7), (10) and (11). In the range of t_0 where ϕ and

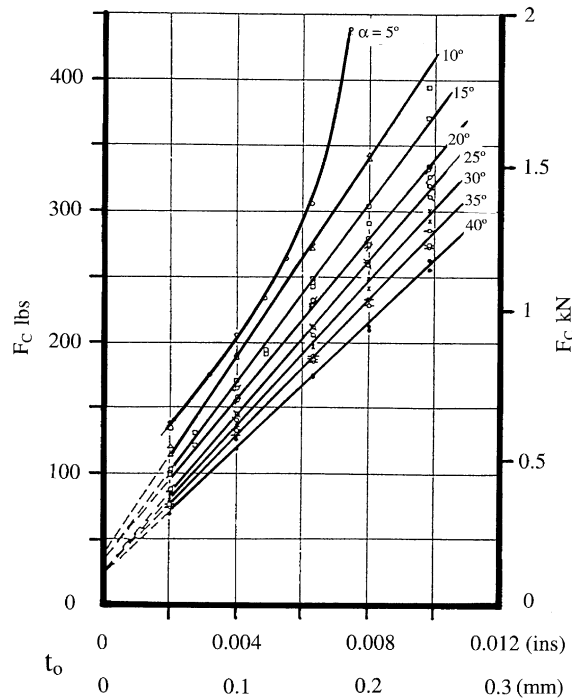


Fig. 5. Cutting force vs. depth of cut for SAE 1112 cold rolled steel (end cutting of tubular specimen, width of cut 0.2 in = 5 mm). (after [29]). The positive intercept has meaning according to the new analysis, connected with the fracture component of work or forces. The non-linear behaviour at small α and large t_0 is because the chips were discontinuous for those conditions.

γ are practically constant, Eq. (7) says that for a given material (R/τ_y), F_C vs. t_0 is linear with slope $[\tau_y w/Q]$ and intercept Rw/Q ; similarly there is a positive F_S intercept in F_S vs. A_S plots, Eq. (10).

A way of proceeding in order to establish the R and τ_y using a spreadsheet is as follows:

- (i) from the F_C and F_V vs. t_0 plots for given rake angle α , establish β from $F_V = F_C \tan(\beta - \alpha)$, Eq. (2);
- (ii) for various Z , find the optimum ϕ values (solution to Eq. (6)) and Q values for the relevant α and associated β found in (i);
- (iii) from the experimental intercept I , calculate the range of candidate R given by IQ/w where w is the width of cut, corresponding with the range of Z chosen in (ii);
- (iv) from the experimental slope S , calculate the range of candidate shear yield stresses τ_y given by $SQ/w\gamma$ for the same range of Z ;
- (v) calculate the intercept/slope ratios I/S at various Z from the *calculated* R and τ_y given in steps (iii) and (iv) and compare with the *experimental* I/S ratio to establish the correct Z ;
- (vi) from the correct Z , the t_0 values may be established and compared to the experimental depths of cut;
- (vii) from the correct Z , read off the correct R and τ_y ;
- (viii) from the correct Z , read off the ϕ and compare with experimental shear plane angles (if known).

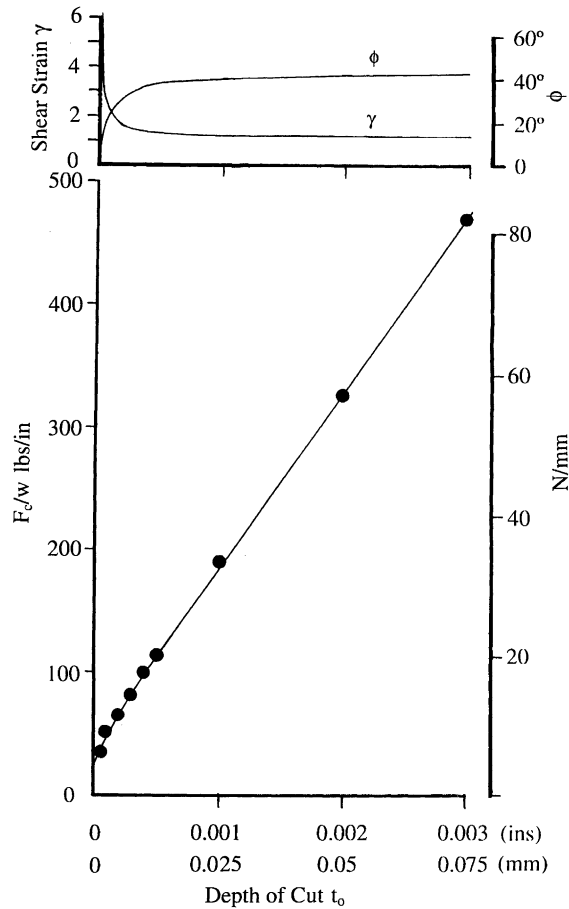


Fig. 6. Cutting force per unit width of cut vs. uncut chip thickness data from Finnie [47] for leaded steel (his Fig. 4). Both the linear region at large t_0 (constant ϕ and γ) and the region curving down towards the origin at small t_0 (changing ϕ and γ) are shown. The line is the prediction of Eq. (6) with $\beta = 37^\circ$ (established from the accompanying F_V data) and $R/\tau_y = 3.6 \times 10^{-4}$ in (10^{-5} m). Since $\tau_y = 68$ ksi (470 MPa) from the analysis, $R = 24$ lbs/in (5 kJ/m²). This is relatively low for R for soft mild steel and suggests that the toughness of free-cutting metals is lower than their 'plain' counterparts. Low toughness, caused by all the particles in the microstructure producing voiding, in addition to the usual factors, would help explain the ease of cutting in these sorts of metals.

These calculations should be repeated for each α , checks being made for systematic changes in the derived parameters. A similar route may be followed when F_S vs. A_S results are being analysed, in which β is first established, then answers for a variety of Z are obtained, the correct one of which is that which makes the experimental and calculated I/S ratios agree (and which gives agreement between the predicted and experimental ϕ if known). Fig. 6 shows the results of such calculations for Finnie's [47] results on the dry cutting of leaded steel with a 35° rake angle/ 5° clearance angle tool. These data have been chosen to illustrate application of the new model, rather than the data in Fig. 5, say, because extremely shallow depths of cut were taken as well as regular-size cuts. In consequence, not only is the 'linear, constant ϕ ' region evident as in Fig. 5, but

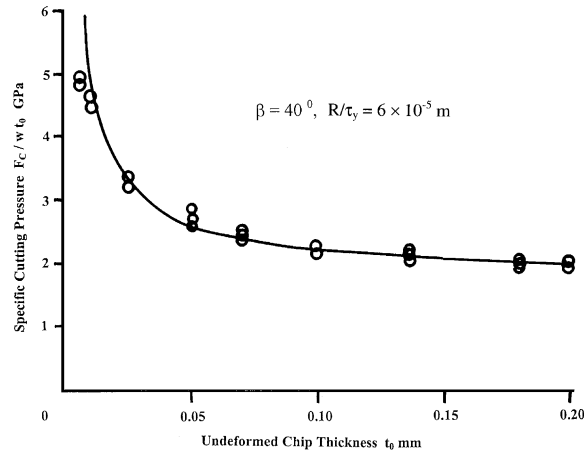


Fig. 7. The size effect in 0.48% plain carbon steel cut with a negative rake tool ($\alpha = -5^\circ$). Data from Kopalinsky and Oxley [49]. The curve is the prediction of the new theory for $\beta = 40^\circ$ and $R/\tau_y = 6 \times 10^{-5}$ m giving $Z = 0.3$ at $t_0 = 0.2$ mm.

also the ‘non-linear, changing ϕ ’ region at small t_0 is clearly shown. Furthermore, the results will highlight the relatively low toughness implied by these results for free-cutting materials. The curve in Fig. 6 is not Finnie’s faired-in curve, but the prediction of Eq. (7) with $\beta = 37^\circ$ (established from the accompanying F_V data) and $R/\tau_y = 3.6 \times 10^{-4}$ in (10^{-5} m). Since $\tau_y = 68$ ksi (470 MPa) from the analysis, $R = 24$ lbs/in (5 kJ/m^2). This is relatively low for R for soft mild steel and suggests that the toughness of free-cutting metals is lower than their ‘plain’ counterparts. Low toughness, in addition to the usual factors, would help explain the ease of cutting in these sorts of metals. Calculations derived some years ago from machining data suggested that the toughness of leaded brass, for example, is about one-fifth of that of unleaded brass; the hardnesses of both are the same [48].

The curve in Fig. 6 does not pass through the origin even though it curves downwards. The intercept at zero uncut chip thickness is still given by $Rw/Q = Rw$ now since $Q = 1$ at zero t_0 (where Z is infinite) as ϕ is zero. This other intercept is an alternative way of estimating (the same) R .

3.3. The size effect in machining

The *size effect* concerns what happens near the origin of F_c vs. t_0 plots where the new model shows that there are reductions in ϕ and increases in γ . Often, the size effect is illustrated by increases in the specific cutting pressure (unit power) given by (F_c/wt_0) at small t_0 . The data points in Fig. 7 demonstrate the size effect in 0.48% plain carbon steel cut with a tool having $\alpha = -5^\circ$ [49]. Inspection of Eq. (9a) explains why the specific cutting pressure must inevitably increase to large values, at small depths of cut, owing to the inverse-dependent $(R/Q)(1/t_0)$ term. The ratio of specific cutting pressures at $t_0 = 0.01$ and 0.2 mm is some 2.5 in Fig. 7. Such a ratio (and the intermediate curve) can be predicted by Eq. (9a) or (9b), using $\beta = 40^\circ$ and $R/\tau_y = 6 \times 10^{-5}$ (which gives $Z_{t_0=0.2 \text{ mm}} = 0.3$) changing Z for other values of t_0 according to $Z_t = (0.2/t)(0.3)$. Reductions in ϕ from the ‘levelled-out’ value at large t_0 (Fig. 3d) increase γ (Fig. 3e). The effect becomes much more significant at small t_0 owing to the inverse dependence of Z on t_0 .

Kopalinsky and Oxley [49] explained the size effect in terms of increasing ϕ with chip thickness: Fig. 8 gives their experimental results for ϕ . The line plotted in Fig. 8 is the prediction of Eq. (6)

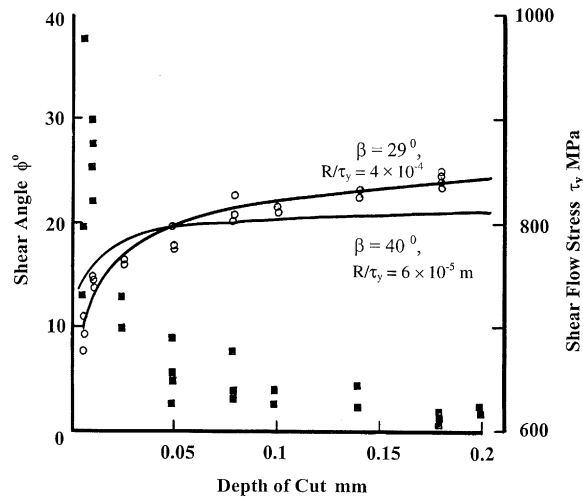


Fig. 8. The reduction of ϕ at smallest depths of cut which gives rise to the size effect in cutting. Data (open circles) from Kopalinsky and Oxley [49]. Curves are predictions of the new analysis for given $\beta = 29^\circ$ and $R/\tau_y = 6 \times 10^{-5}$ m. Filled square data points are τ_y derived by Kopalinsky and Oxley using the increase cutting forces along the shear plane. Values change and are artificially high because of the positive intercept in plots of F_c vs. t_0 or F_S vs. A_S . The new analysis is able to predict the behaviour using constant $\tau_y = 391$ MPa.

using $\beta = 40^\circ$ and $R/\tau_y = 6 \times 10^{-5}$, as employed in Fig. 7. The agreement is acceptable but an even better fit is shown with $\beta = 29^\circ$ and $R/\tau_y = 4 \times 10^{-4}$ (there is no information for β in the original paper). However the rise in specific cutting pressure is too large with this combination of parameters and does not agree with experiment. We note however that it is *not necessary* for ϕ to reduce with t_0 for the curve of (F_c/wt_0) to rise at small t_0 (see Eq. (9a)).

Another explanation advanced for the size effect relates to the greater probability of not encountering a defect at small depths of cut, thus making cutting more difficult. Undoubtedly there comes a time when uncut chip thicknesses may be comparable with microstructural features when application of a continuum theory must be in doubt. But size effects are well known in fracture mechanics, and come about because the surface (fracture) work depends upon *area* whereas the gross plastic flow (chip work) depends upon *volume*, so the terms scale differently (it is a cube-square scaling phenomenon (see, e.g. [44, Chapter 9])). It is perhaps significant that the non-dimensional parameter $R/\tau_y t_0 \gamma = Z/\gamma$ employed in this paper is related to the parameter $\xi = (\int \sigma d\epsilon/R)(V/A)$ used in scaling problems in plastic fracture mechanics, Atkins [50]. (V/A) is the ratio of plastic volume to crack area, which is t_0 in machining with a single shear plane. Hence for a non-workhardening material $Z/\gamma = 1/\xi$. Also we note that $Z = R/\tau_y t_0 = 2m\delta_c/t_0$ where m ($1 < m < 3$, say) is the constraint factor and δ_c is the critical crack opening displacement (COD) of fracture mechanics [20]. Z is therefore a ratio of COD to uncut chip thickness. A similar ratio was discussed by Atkins [48,51].

3.4. Anomalously high τ_y at small t_0

Also in Fig. 7 are Kopalinsky and Oxley's derived values of τ_y on the primary shear plane. The values of τ_y were found by dividing the component of measured forces along the primary shear plane

by the area of the plane given by the corresponding experimental value of ϕ which, in turn, had been determined in the usual way from chip geometry using measured chip thicknesses. The values for τ_y were *not* derived from the *slope* of an F_c vs. t_0 plot but from separate (F_c, t_0) data points. Kopalinsky and Oxley's values of τ_y vary with t_0 and take values of nearly 1000 MPa at the smallest depth of cut, and 600 MPa at the largest. The reason why Kopalinsky and Oxley's derived τ_y rise to very high values at small t_0 is because the F_c – t_0 relation does not pass through the origin (Eq. (7)) as assumed in their method of calculation. At small t_0 the intercept becomes a significant proportion of F_c (and of F_S in a corresponding F_S – A_S diagram). Anomalously high values of τ_y *must* result.

For $\beta=40^\circ$ and $R/\tau_y=6 \times 10^{-5}$, the theoretical (F_c/t_0w) at $t_0=0.2$ mm in Fig. 7 is $5.4\tau_y$ according to Eq. (9). The experimental value is 2111 MPa, whence $\tau_y = 391$ MPa, and has that *same* value all along the rising curve. (This is lower than Kopalinsky and Oxley's lowest τ_y of 600 MPa and we note that their specific cutting pressures in Fig. 7 have not levelled-out at their greatest t_0 : their Z is still above the threshold value of ca. 0.1). The theory presented in this paper is capable of explaining the whole F_c/wt_0 vs. t_0 size effect behaviour with a *constant* τ_y of about 391 MPa rather than the changing, and very high, τ_y values usually given in the literature.

The new model for metal cutting is compatible with empirical relations between unit power and depth of cut (see [52]). For example, Shaw and Oxford [53] showed that the specific cutting energy varied inversely with $t_0^{0.2}$. Log plotting of the curve predicted by Eq. (9) shows that, over a practical range of t_0 , such a power-law representation is adequate.

When the cutting speed is increased, with all other parameters kept constant, the specific cutting force for many materials falls. Fig. 9 reproduces data from Childs et al [54, Fig. 3.6]. The plots are like Figs. 7 and 8 but where the abscissa is speed rather than depth of cut. Materials illustrated are commercially pure aluminium, copper, iron, nickel and titanium; copper and aluminium alloys; carbon and low alloy steels; austenitic steels; and nickel and titanium alloys. Accompanying these data are the corresponding ϕ values which increase with increase in speed, in the same way that ϕ increases with depth of cut (Fig. 3d). The reduction in unit power, and the increase in ϕ , depends on the material. Taken together, this means that speed reduces the Z values and, at constant depth of cut, R/τ_y decreases with increase of speed. Calculations for these data are performed in the next section.

Higher cutting speeds mean higher strain rates. Broadly speaking the flow stresses of mild steel, some aluminium alloys (though not precipitation hardened alloys) and titanium are rate sensitive, whereas magnesium alloys and copper show little rate sensitivity. The increase in τ_y with speed would explain reductions in Z if R were to remain constant with speed, but it is expected as well that R decreases with increase of rate, whence Z would reduce even more quickly. Since copper (whose τ_y is *not* usually considered to be rate dependent) displays a reduction in specific cutting force and increase in ϕ with cutting speed, it suggests that R for copper must decrease with rate (see the following section).

3.5. Effect of thermomechanical treatment on R/τ_y

R/τ_y will change with thermomechanical treatment of metals. It might be expected that cold worked materials would have lower R and greater hardness (greater τ_y) than when annealed. In Section 3.2, the R/τ_y ratio for Eggleston et al.'s [45] SAE 1112 steel was calculated to be $50 \text{ kJ/m}^2/100 \text{ MPa} = 5 \times 10^{-4} \text{ m}$ (annealed) and $40 \text{ kJ/m}^2/200 \text{ MPa} = 2 \times 10^{-4} \text{ m}$ (cold rolled). The toughness-to-strength ratio is, in this material, reduced by cold working. Reduction in R/τ_y and hence reduction in Z at a

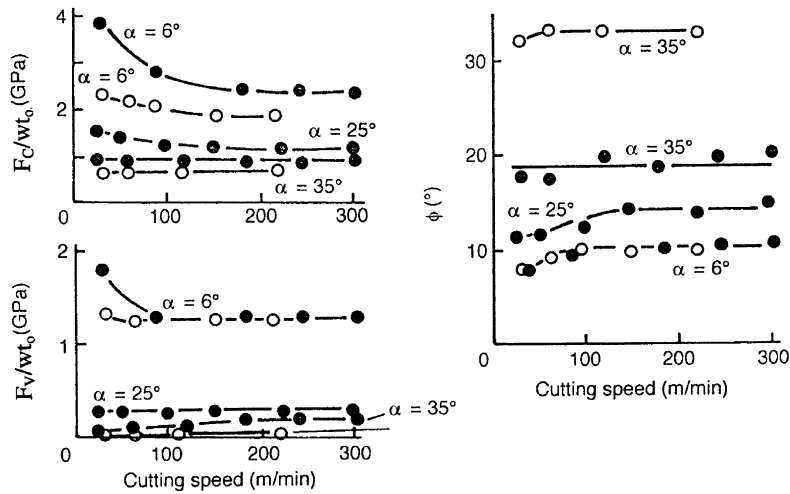


Fig. 9. Reductions in specific cutting force with speed for annealed (filled points) and prestrained (open points) commercially-pure copper from tests with uncut chip thicknesses between 0.15 and 0.2 mm (after [54]). Also shown are the changes in primary shear plane angle ϕ . Calculations using the new model give $Z_{\text{annealed}} = 8.9$ and $Z_{\text{prestrained}} = 1.5$ which translates to $R/\tau_y = 1.8 \times 10^{-3}$ (annealed) and 3×10^{-4} (prestrained). This shows that the toughness-to-strength ratio is smaller in workhardened copper and that since copper is not particularly strain rate sensitive, the toughness must decrease with speed.

given t_0 , increases the shear plane angle ϕ , Fig. 3. When ϕ_{annealed} is low ($< 40^\circ$, say), an increased $\phi_{\text{cold worked}}$ produces a *reduction* in γ (Fig. 3e) and hence a reduction in cutting force according to Eq. (6). Kopalinsky and Oxley comment on ‘the somewhat paradoxical result of reducing cutting forces by cold working a material so that its hardness is increased’. They attributed the effect to a balance between the increase in ϕ giving a reduced length of primary shear zone and the increase in τ_y caused by work hardening affected by rate and temperature, but the new analysis says that it is to be expected at constant yield stress when surface work is included. Kopalinsky and Oxley [55] note that in higher carbon steels, the effect is less noticeable or even reversed (i.e. cold worked material requires greater cutting forces than annealed). Since higher carbon steels, even in the annealed condition, will have lowish R/τ_y , ϕ_{annealed} will be greater than for softer steels, other things being equal. When ϕ_{annealed} is greater than about 40° , increasing ϕ produces an increase in γ particularly at small α . (see Fig. 3.4 in [56].) F_c is then predicted to increase, Eq. (8), exactly as observed by Kopalinsky and Oxley [55].

Data in Childs et al. [54] on commercially pure copper (reproduced as Fig. 9 here) lend support to the idea of R/τ_y being smaller for workhardened materials. Using their ϕ data for cutting with $\alpha = 35^\circ$, the new model suggests $Z_{\text{annealed}} = 8.9$ and $Z_{\text{prestrained}} = 1.5$. For (0.15–0.2) mm feed rates, this gives R/τ_y as 1.8×10^{-3} (annealed) and 3×10^{-4} (prestrained).

3.6. Proportions of total work due to plasticity, friction and fracture

It is reasonable to ask what are the proportions of total work or cutting force attributable to plasticity, friction and fracture, particularly since work of fracture has previously been considered insignificant. Table 1 gives some representative values for different cutting conditions.

Table 1

α	Z	β	Plasticity (%)	Friction (%)	Fracture (%)
-5°	0.1	0	99	0	1
-5°	0.1	57°	54	44	1
-5°	10	0	24	0	76
-5°	10	57°	28	29	43
$+10^\circ$	0.1	0	94	0	6
$+10^\circ$	0.1	57°	53	45	2
$+10^\circ$	1	0	64	0	36
$+10^\circ$	1	57°	43	43	15
$+10^\circ$	10	0	22	0	78
$+10^\circ$	10	57°	8	77	15

It is clear that the percentages vary with conditions, and that fracture work may, or may not, be an appreciable percentage of total cutting work or force. Note that the parameter Z combines both the material property R/τ_y and the uncut chip thickness t_0 , so that for a given material, deeper cuts involve a smaller proportion of fracture work and a larger proportion of plastic work. Why, if work of surface formation can be significant, considerable progress has been made over the past half-century in understanding machining by ignoring it, is discussed in Section 4 later. Again, why fracture is important in continuous chip machining, even in the absence of tool tip cracks, is also discussed in Section 4.

3.7. R/τ_y ratios; R and τ_y values

Table 2 brings together the material properties R and τ_y determined above. Sensible, consistent, values for R/τ_y of some 10^{-5} – 10^{-4} m are predicted by the new analysis from the wide body of experimental data in the literature for ductile metals. Similar values are obtained from all the different methods of analysis discussed in the paper (i.e. ϕ values, $F_c - t_0$ or $F_S - A_S$ plots, size effect etc. for a given material in a given thermomechanical state). While τ_y is known to increase with strain rate for some metals, there is little information available on the effect of strain rate on ductile R values: even so Table 2 suggests, perhaps not unexpectedly, that R in cutting is less than quasi-static values where known. Some authors of FEM papers have employed separation criteria that alter with temperature (e.g. Liu and Guo, [6]).

A criticism of the present paper is, perhaps, that there are no new machining data presented for materials for which independent mechanical properties (particularly toughness) have been obtained. That is currently being redressed at Reading with a programme of cutting a wide range of well-characterised materials, and will be reported in the future. First results show agreement with the ideas presented here.

4. Discussion

Traditional ‘plasticity and friction only’ analyses of machining have been able to make progress in the past half-century in the understanding of chip flow, chip curl, built-up edge formation, tool

Table 2
From machining experiments

Materials	R/τ_y (m)	τ_y (MPa)	R (kJ/m ²)	Independent quasi-static $R^{a,b}$ (kJ/m ²)
Annealed SAE 1112 steel ^c	4×10^{-5}	445	18	200
Cold worked SAE 1112 steel ^c	3×10^{-5}	571	16	200
“Mild steel” ^d	6×10^{-4}	—	—	300
“Steel” ^e	3×10^{-3}	—	—	—
SAE 4135 steel ^f	3×10^{-5}	570	18	60
NE 9445 steel ^g	2×10^{-5}	583	14	—
SAE 1015 steel ^h	4×10^{-5}	683	24	—
2024-T4 aluminium alloy ^c	2×10^{-5}	350	6	15
6061-T6 aluminium alloy ^c	3×10^{-5}	239	7	30
“Aluminium” ^d	5×10^{-3}	—	—	—
“Aluminium” ^e	2×10^{-3}	—	—	—
85/15 cold drawn brass ^c	3×10^{-5}	354	11	250
“Brass” ^e	6×10^{-4}	—	—	—
“Cast iron” ^e	3×10^{-4}	—	—	—
“Copper” ^d	4×10^{-3}	—	—	—
Annealed copper ⁱ	2×10^{-3}	—	—	830
Coldworked copper ⁱ	3×10^{-4}	—	—	650
Tin ^c	7.5×10^{-3}	—	—	—
Lead ^c	1.5×10^{-2}	—	—	75

Except where indicated, the references are those given in this paper.

^aLatzko and Turner [21]

^bBlyth (2002), (private communication)

^cKobayshi and Thomsen [29]

^dPugh [38]

^eOkoshi [45]

^fCreveling et al. (1957): see [29]

^gMerchant [36]

^hKececioglu (1958): see [29]

ⁱChilds et al. [54] (friction angle not reported, therefore some uncertainty)

stresses and tool temperatures etc. without regard to work of surface separation [57–59]. It is proper to ask how this can be, if surface work is so important.

Given that the single shear plane model does not reflect the more complicated primary and secondary shear zones found in the practical cutting of workhardening ductile metals, it is understandable that all the painstaking investigations of practical flow fields must lead to a better understanding of

chip flow. With a predetermined parting line (the machined surface) the geometry of plastic flow can be investigated without regard to whether the formation of that surface requires a small or large amount of work. The studies of parallel-sided shear zones, workhardening slip line field analyses with primary and secondary shear zones, the effects of large strain, strain rates and temperatures and cutting speed etc., the replacement of simple Coulomb friction with more realistic treatments of stick-slip tool-workpiece friction, have all contributed to a better understanding of machining. Indeed, as mentioned in Section 1, the predictions of the present model would undoubtedly be improved were the plastic work of more realistic flow fields, and were better friction models, to be incorporated along with the significant surface work.

Nevertheless, at the simplest level, it remains the case that there is no ‘algebraic’ theory for metal cutting that predicts a material-dependent primary shear plane angle ϕ and all that follows from that. In consequence, empirical relations are still often used for cutting forces and power, and for tool life from tool stresses and temperatures (e.g. [52]). Even the advent of FEM does not provide all the answers, owing to the arbitrariness of some of the separation criteria associated with the formation of new surfaces that are employed in the FEM models. This paper notes that separation criteria should reflect the physics of new surface formation, and that when they do, specific surface works of kJ/m^2 are found in FEM models (rather than the J/m^2 employed those years ago by Shaw) and that surface work can be a large percentage of the total FEM cutting work. The reason that it has never been found necessary to incorporate surface work of such magnitude in traditional machining theories is that they are derived from force equilibrium where work components are not separately identified, and where uncertainties about friction and flow stresses, at the high rates and temperatures found in metal cutting, allow ‘agreement’ between analysis and experiment to be obtained.

Furthermore, although FEM analysis may be the preferred ‘modern’ way of modelling machining, each solution is for a particular set of conditions with a particular metal and it is difficult to establish general trends without running a very large number of cases. The new algebraic model, however imperfect, does enable useful generalizations to be made.

The major contribution of the new analysis is its ability to predict material-dependent primary shear plane angles θ and its interpretation of experimental cutting forces and power. The new theory finds no disagreement with the traditional method of determining shear yield stresses from the slopes of F_S vs. A_S diagrams, but it does give a meaning for the ignored positive force intercepts invariably found in such plots (and in F_C vs. t_0 plots), cf. Eqs. (9)–(11), which are measures of the toughness. It explains the size effect quantitatively and shows why anomalously high flow stresses have been reported for that range of operation having small uncut chip thicknesses. According to the new model, the actual shear yield stress is not greater at small t_0 and has the same value as for deeper depths of cut.

The toughness/strength (R/τ_y) ratio, rather than τ_y alone, controls machining behaviour at a given depth of cut. Thermomechanical treatment will alter this ratio, increase of τ_y usually being accompanied by a reduction in R . This is why hardness alone is insufficient to characterise cutting behaviour. Furthermore, the effect of strain rate and temperature on R and on τ_y may not always be ‘in the same direction’ which gives rise to difficult-to-understand experimental machining behaviour when interpreted in terms of yield stress alone. Childs et al. [54, p. 88] state that ‘the reason for the easier machining of [copper and aluminium] alloys compared with the elemental metals is not obvious from their room temperature, low strain rate mechanical behaviours [which are very similar]’ According to this paper the reason is bound up in different toughness R values.

5. Conclusions

Incorporation of significant surface work in the basic Ernst–Merchant metal cutting theory at the kJ/m^2 levels expected on the basis of modern ductile fracture mechanics predicts that:

- (i) (as long known from experiments) The primary shear plane angle ϕ depends on material as well as tool rake angle α and friction. No previous analysis has been able to do this.
- (ii) The primary shear plane angle ϕ depends on undeformed chip thickness at very small t_0 and shows how ϕ increases to ‘levelled-out’ values at larger t_0 . Again, this is confirmed by experiment.
- (iii) The controlling material-dependent parameter is the toughness-to-strength ratio R/τ_y , which is combined with the uncut chip thickness in the new analysis to form a non-dimensional parameter $Z = R/\tau_y t_0$.
- (iv) The positive intercepts found in plots of cutting force F_c vs. depth of cut t_0 , or plots of force resolved along the shear plane F_S vs. the area of the shear plane A_S . The intercepts are (different) measures of the fracture toughness R .
- (v) The experimentally observed large increases in specific cutting pressure (unit power), given by F_C/wt_0 , at small t_0 are inevitable according to the new analysis since unit power depends inversely on t_0 .
- (vi) The very large values of τ_y at small t_0 reported in the literature from experiments investigating variations in specific cutting force with t_0 , are artificially large owing to neglect of the finite intercepts in plots of F_C vs. t_0 or F_S vs. A_S . That is, τ_y is calculated from individual (F_S , A_S) data points as if they passed through the origin, rather than from the slopes of the actual F_S vs. A_S plots.
- (vii) The work of fracture can be a significant component of total cutting work under certain conditions (including many practical cases of cutting ductile metals).
- (viii) The material toughness/strength ratio (R/τ_y) will depend upon material chemistry and prior thermomechanical treatment, as well as strain rate and temperature during cutting. Since R/τ_y usually decreases in harder workpieces, an explanation is given for why workhardened samples are sometimes easier to cut than annealed workpieces of the same metal.
- (ix) If rate and temperature effects produced by changes in cutting speed change the (R/τ_y) ratio in materials, this will lead to reductions in specific cutting force with speed when, as seems usually the case, R/τ_y falls with increase of rate.
- (x) The ‘separation criterion’ required in FEM modelling of cutting ought to reflect closely the physics of separation at the tool tip to give most realistic simulations, rather than be a ‘computational fix’[60].

Acknowledgements

I am grateful to T.H.C. Childs, B. Cotterell and F.A. McClintock for helpful discussions on the link between machining and ductile fracture mechanics.

References

- [1] Astakhov VP. *Metal cutting mechanics*. Boca Raton, FL: CRC Press, 1999.
- [2] Shaw MC. *Metal cutting principles*, 3rd ed. Cambridge, MA: MIT Press, 1954.
- [3] van Luttervelt CA, Childs THC, Jawahir IS, Flocke F, Venuvinod PK. Progress report of the CIRP working group ‘Modelling of Machining Operations’. *Annals CIRP* 1998;47:587–626.
- [4] Camatini E. A systematic research on the cold work produced on carbon steels by machining on a lathe. *Proceedings of the Eighth MTDR Conference, UMIST Part 1*. 1967. p. 565–90.
- [5] Yang X, Liu CR. A new stress-based model of friction behaviour in machining and its significant impact on residual stresses computed by finite element method. *International Journal of Mechanical Sciences* 2002;44:703–23.
- [6] Lin CR, Guo YB. Finite element analysis of the effect of sequential cuts and tool-chip friction on residual stresses in a machined layer. *International Journal of Mechanical Sciences* 2000;42:1069–86.
- [7] Strenkowski JS, Carroll III JT. A finite element model of orthogonal metal cutting. *ASME Journal of Engineering for Industry* 1985;107:349–54.
- [8] Carroll III JT, Strenkowski JS. Finite element models of orthogonal cutting with application to single point diamond turning. *International Journal of Mechanical Sciences* 1988;30:899–920.
- [9] Lin Z-C, Lo S-P. A study of deformation of the machined workpiece and tool under different low cutting velocities with an elastic cutting tool. *International Journal of Mechanical Sciences* 1998;40:663–81.
- [10] Komvopoulos K, Erpenbeck SA. Finite element modeling of orthogonal metal cutting. *ASME Journal of Engineering for Industry* 1991;113:253–67.
- [11] Shih AJ. Finite element simulation of orthogonal metal cutting. *ASME Journal of Engineering for Industry* 1995;117:84–91.
- [12] Usui E, Shirakashi T. *Mechanics of machining—from ‘Descriptive’ to ‘Predictive’ theory. On the Art of Cutting Metals—75 Years Later*, ASME PED-vol. 7, 1982. p. 13–5.
- [13] Zhang B, Bagchi A. Finite element simulation of chip formation and comparison with machining experiment. *ASME Journal of Engineering for Industry* 1994;116:289–97.
- [14] Marusich TD, Ortiz M. Modelling and simulation of high speed machining. *International Journal for Numerical Methods in Engineering* 1995;38:3675–94.
- [15] Huang JM, Black JT. An evaluation of chip separation criteria for the FEM simulation of machining. *Transactions of the ASME Journal of Manufacturing Science and Engineering* 1996;118:545–53.
- [16] Felbeck DK, Atkins AG. *Strength and fracture of engineering solids*. Upper Saddle River, NJ: Prentice-Hall, 1996.
- [17] Griffith AA. The phenomena of rupture and flow in solids. *Philosophical Transactions of the Royal Society* 1921;A221:163–98.
- [18] Griffith AA. The theory of rupture. *Proceedings of the First International Conference on Applied Mechanics, Delft*, 1924. p. 55–63.
- [19] Obreimoff JW. *Proceedings of the Royal Society* 1930;A127:290.
- [20] Knott JF. *Fundamentals of fracture mechanics*. London: Butterworth & Co., 1973.
- [21] Latzko DGH, Turner CE, editors. *Post yield fracture mechanics*, 2nd ed. Barking: Applied Science Publishers, 1984.
- [22] McClintock FA. *Transactions of the ASME Journal of Applied Mechanics* 1968;35:363.
- [23] Rice JR, Tracey DM. *Journal of the Mechanics and Physics of Solids* 1969;17:201.
- [24] Miller KJ. *Structural Integrity—whose responsibility?’ The 36th John Player Lecture. ProcIMechE London: I MechE*, 2001.
- [25] Kendall K. *Molecular adhesion and its applications*. New York: Kluwer Academic/Plenum Publishers, 2001.
- [26] Bikerman JJ. *Physics Status Solidi* 1965;10:3–26.
- [27] Atkins AG. *Ductile shear fracture mechanics. Key Engineering Materials* 2000;177–180:59–68.
- [28] Shaw MC. A new mechanism of plastic flow. *International Journal of Mechanical Sciences* 1980;22:673–86.
- [29] Kobayashi S, Thomsen EG. Some observations on the shearing process in metal cutting. *Journal of Engineering for Industry* 1959;81:251–62.
- [30] McClintock FA. Slip line field fracture mechanics; a new regime of fracture mechanics. In: Reuter WG, Piascik RS, editors. *Fatigue and fracture mechanics: 33rd vol. ASTM STP, 1417*. Philadelphia; ASTM, 2002.
- [31] Piispanen V. Eripaines Teknilliseslä Aikakauslehdeslä 1937;27:315 (see Piispanen V, *Journal of Applied Physics* 1948;19:876.).

- [32] Mallock A. The action of cutting tools. *Proceedings of the Royal Society* 1881;XXXIII:127–39.
- [33] Cook NH, Finnie I, Shaw MC. Discontinuous chip formation. *Transactions of the ASME* 1954;76:153–62.
- [34] Boothroyd G. *Fundamentals of metal machining and machine tools*. McGraw-Hill, NY: Scripta Book Co., 1975.
- [35] Merchant ME. Basic mechanics of the metal cutting process. *Journal of Applied Mechanics* 1944;11:A168–75.
- [36] Merchant ME. Mechanics of the metal cutting process. II. Plasticity conditions in orthogonal cutting. *Journal of Applied Physics* 1945;16:318–24.
- [37] Sata T. Recent developments concerning cutting mechanics. *Proceedings of the International Production Engineering Research Conference*, Pittsburgh, Penna. New York: ASME, 1963. p. 18–25.
- [38] Pugh HLID. Mechanics of the cutting process. *Proceedings of the Institute of Mechanical Engineering Conference on Manufacturing*, Paper 53, 1958. p. 237–54.
- [39] Hill R. The mechanics of machining: a new approach. *Journal of Mechanics and Physics of Solids* 1954;3:47–53.
- [40] Childs THC. Private communication, 2001.
- [41] Stephenson DA, Agapiou JS. *Metal cutting theory and practice*. New York: Marcel Dekker, 1997.
- [42] Oxley PLB. *Mechanics of machining: an analytical approach to assessing machinability*. Chichester, UK: Ellis Horwood, 1989.
- [43] Brown RH, Amarego EJA. Oblique machining with a single cutting edge. *International Journal of Machine and Tool Design Research* 1964;14:9–25.
- [44] Atkins AG, Mai Y-W. *Elastic and plastic fracture*. Chichester, UK: Ellis Horwood, 1985 and 1988.
- [45] Okoshi M. Researches on the cutting force. *Proceedings of the World Engineering Congress*, Tokyo, Japan, Paper 634, 1929. p. 179–205.
- [46] Eggleston DM, Herzog R, Thomsen EG. Observations on the angle relationships in metal cutting. *ASME Journal of Engineering for Industry* 1959;81:263–79.
- [47] Finnie I. A comparison of stress strain behaviour in cutting with that in other material tests. *Proceedings International Production Engineering Research Conference*, Pittsburgh, Penna. New York: ASME, 1963. p. 76–82.
- [48] Atkins AG. Fracture toughness and cutting. *International Journal of Production Research* 1974;12:263–74.
- [49] Kopalinsky EM, Oxley PLB. Size effects in metal removal processes. *Institute of Physics Conference Series No 70, Third Conference on Mechanics Props at High Rates of Strain*, Oxford, 1984. p. 389–96.
- [50] Atkins AG. Scaling in combined plastic flow and fracture. *International Journal of Mechanical Sciences* 1988;30:173–91.
- [51] Atkins AG. A dimensional analysis for machining to include fracture toughness. *Proceedings of 2nd North American Metalworking Research Conference*, Madison, Wis. Dearborn: Society of Manufacturing Engineers, 398–407, 1974.
- [52] ASME Research Committee on Metal Cutting: Data and Bibliography. *Manual on cutting of metals*. New York: ASME, 1952.
- [53] Shaw MC, Oxford CJ. *Transactions of the ASME* 1957;79:139–49.
- [54] Childs THC, MacKawa K, Obikawa T, Yamane Y. *Metal cutting*. London: Arnold, 2000.
- [55] Kopalinsky EM, Oxley PLB. Predicting the effects of cold working on the machining characteristics of low carbon steels. *ASME Journal of Engineering for Industry* 1987;109:257–64.
- [56] Trent EM. *Metal cutting*, 3rd ed. Stoneham, MA: Butterworth-Heinemann, 1991.
- [57] Shaw MC. *Metal cutting principles*. Oxford: Oxford University Press, 1984.
- [58] Thomsen EG, Yang CT, Kobayashi S. *Mechanics of plastic deformation in metal processing*. New York: Macmillan, 1965.
- [59] Zorev NN. *Metal cutting mechanics (translated JSJ Massey)*. Oxford: Pergamon, 1966.
- [60] Atkins AG. Fracture mechanics and metalforming: damage mechanics and the local approach of yesterday and today. In: Rossmannith HP editor, *Fracture research in retrospect*. Rotterdam; FL: Balkema, 1998.